
Princeton Plasma Physics Laboratory

PPPL-

PPPL-



Prepared for the U.S. Department of Energy under Contract DE-AC02-09CH11466.

Princeton Plasma Physics Laboratory

Report Disclaimers

Full Legal Disclaimer

This report was prepared as an account of work sponsored by an agency of the United States Government. Neither the United States Government nor any agency thereof, nor any of their employees, nor any of their contractors, subcontractors or their employees, makes any warranty, express or implied, or assumes any legal liability or responsibility for the accuracy, completeness, or any third party's use or the results of such use of any information, apparatus, product, or process disclosed, or represents that its use would not infringe privately owned rights. Reference herein to any specific commercial product, process, or service by trade name, trademark, manufacturer, or otherwise, does not necessarily constitute or imply its endorsement, recommendation, or favoring by the United States Government or any agency thereof or its contractors or subcontractors. The views and opinions of authors expressed herein do not necessarily state or reflect those of the United States Government or any agency thereof.

Trademark Disclaimer

Reference herein to any specific commercial product, process, or service by trade name, trademark, manufacturer, or otherwise, does not necessarily constitute or imply its endorsement, recommendation, or favoring by the United States Government or any agency thereof or its contractors or subcontractors.

PPPL Report Availability

Princeton Plasma Physics Laboratory:

<http://www.pppl.gov/techreports.cfm>

Office of Scientific and Technical Information (OSTI):

<http://www.osti.gov/bridge>

Related Links:

[U.S. Department of Energy](#)

[Office of Scientific and Technical Information](#)

[Fusion Links](#)

Energy-resolved x-ray imaging for magnetically confined fusion plasmas: measurement of impurity concentration and thermal and non-Maxwellian electron distributions

L. Delgado-Aparicio¹, K. Hill¹, N. Pablant¹, M. Bitter¹, P. Efthimion¹, B. Stratton¹, A. Diallo¹, J. Menard¹, S. Gerhardt¹, D. Gates¹, R. Kaita¹, D. Johnson¹, R. Wilson¹, R. Hawryluk¹, R. Granetz², J. Rice², D. Stutman³, K. Tritz³, E. Hollman⁴ and R. Boivin⁵

¹Princeton Plasma Physics Laboratory, Princeton, NJ, 08540
²MIT – Plasma Science and Fusion Center, Cambridge, MA, 02139
³The Johns Hopkins University, Baltimore, MD, 21218
⁴University of California at San Diego, San Diego, CA, 92093
⁵General Atomics, San Diego, CA, 92121

Abstract

X-ray imaging of magnetically confined fusion (MCF) plasmas in multiple energy ranges offers the opportunity of measuring, simultaneously, various important plasma properties. The space, time and energy-resolved measurements can be used to produce images of impurity concentrations (n_Z and Z_{eff}) - from the absolute image intensity at different energy bands - and the electron energy distribution function, both thermal (T_e) and non-Maxwellian ($n_{e,nM}$) - from the variation of emissivity with x-ray energy. This capability also enables the study of the formation of RF-driven non-Maxwellian “tails” (e.g. ECRH, ECCD and LHCD) and the production of anisotropic hard x-ray distributions during electron runaway generation and its mitigation.

I. Background and motivation

Thanks to important advances in the x-ray detector technology, especially, the manufacturing of two-dimensional hybrid pixel array x-ray detectors of large areas and high count rate capabilities, it is now possible to record spatially resolved x-ray photons at multiple energy ranges from highly charged ions from tokamak plasmas. Previous attempts to develop this capability in the soft x-ray (SXR) energy range have lacked temporal, spatial or energy-resolution. Single-chord pulse-height-analyzers (a.k.a. PHA, see Figs. 1 and 2 and refs [1-5]) are naturally restricted since they are line-integrated measurements with limited spatial localization (e.g. one spectrum per instrument and with very poor profile definition). A schematic drawing of the system prototyped in the Princeton Divertor Experiment (PDX) with five SiLi detectors [1] is depicted in Fig. 1. The traditional PHA diagnostic uses thin silicon-based detectors to obtain slow (≥ 50 -500 ms) time-resolved x-ray spectroscopy of core plasmas emitting photon energies in the 1-20 keV range.

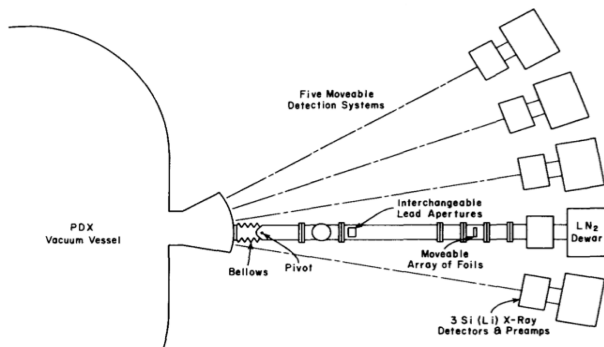


Fig. 1. Schematic of the multi-detector PHA system designed for Princeton Divertor Experiment (PDX [1]) with detail view of the tube assemblies.

The typical spectra obtained are shown in Fig. 2, and consist of an exponentially decreasing continuum due to plasma and impurity Bremsstrahlung and recombination emission with a characteristic $S(E)=S_0\exp(-E/k_B T)$ emission, and distinctive x-ray peaks from impurity ions. Medium-Z impurity concentrations (e.g., Ti, Cr, Fe, Ni) are derived from the intensity of the impurity peaks by use of theoretical plasma-electron-excited x-ray production rates. These rates must be averaged over the expected distribution of charge states of an impurity, since the PHA

cannot resolve these charge states. Because the continuum is a well-known function of T_e , an average core electron temperature $\langle T_e \rangle$ along a line-of-sight can be derived from the measured spectrum; an example of the latter is highlighted in Fig. 2. The complexities associated with using arrays of liquid-nitrogen (LN_2), cooled Si(Li), and H α Ge x-ray detectors (shown in Fig. 1 and refs [1-5]) have nowadays been lifted by using individual silicon-drift-detectors (SDDs, see for e.g. refs. [6,7]). Nonetheless, the time- and space-resolution are still very limited.

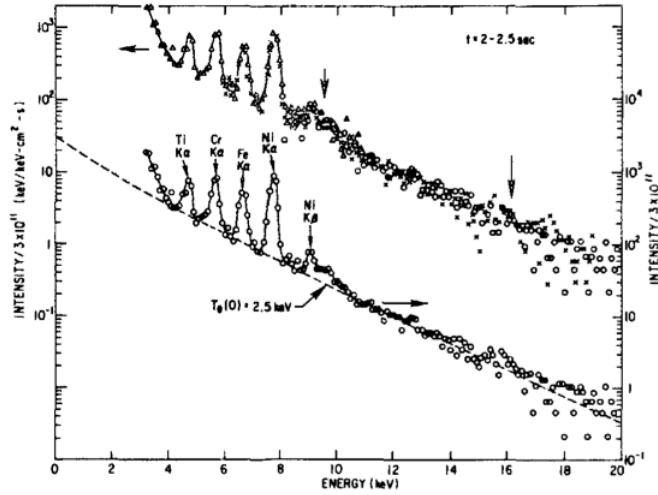


Fig. 2. Spectra from the Tokamak Fusion Test Reactor (TFTR [2]) plasma as measured by three detectors of the x-ray pulse-height analysis (PHA) system.

A better spatial coverage at the expense of a lack of energy resolution can be gained using multiple 1D pin-hole x-ray detector arrays filtered using individual metallic foils (see Fig. 3 and ref. [8]). By using multiple foils with different cut-off energies (E_C) and several detectors with identical plasma views, it is possible to probe the same plasma volume [see Fig. 3-a)] at multiple energy ranges. The electron temperature shown in Fig. 3-b) is obtained by modeling the slope of the continuum radiation from ratios of the available 1D-Abel inverted radial emissivity profiles over different energy ranges, with no *a priori* assumptions of plasma profiles, magnetic field reconstruction constraints or need of shot-to-shot reproducibility. In this case, the multi-energy-inferred electron temperature profile shows a shorter time resolution (≤ 1 ms) in comparison to that of the multi-point Thomson scattering diagnostic (16 ms). This technique has been used to perform fast

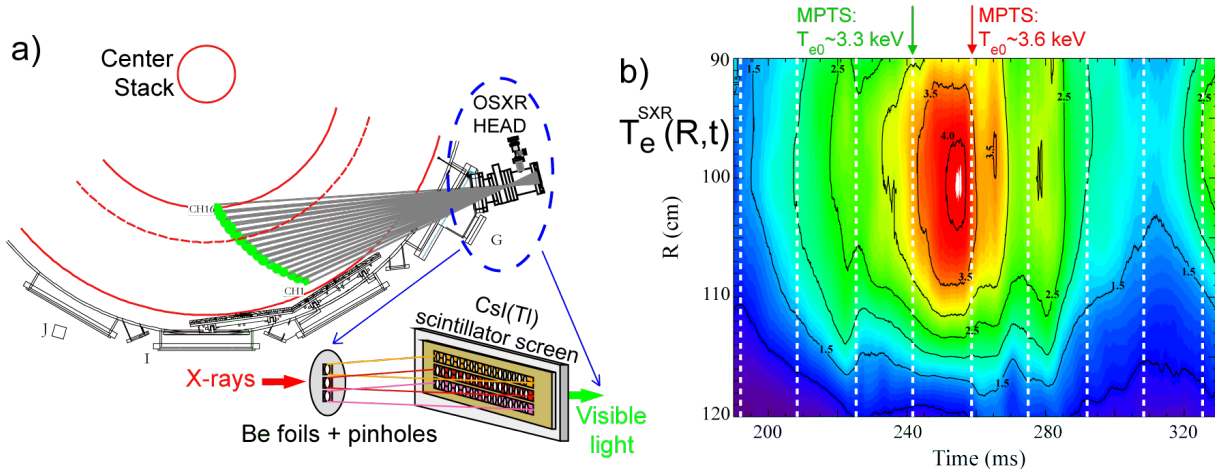


Fig. 3. a) Tangential geometry for the 3-color (foil) multi-energy OSXR array in NSTX; the three set of detectors at each horizontal location have nearly identical plasma views [8]. b) The SXR-inferred $T_e(R,t)$ profile indicates a core temperature up to 4.1 ± 0.2 keV “bracketed” by maximum core Thomson scattering measurements (indicated by the white dotted lines) of 3.3 and 3.6 keV.

electron temperature measurements in the National Spherical Torus Experiment (NSTX), avoiding the time and magnetic-field limitations and requirements imposed by the well-known multi-point Thompson scattering and electron cyclotron emission (ECE), respectively. The electron Bernstein wave (EBW) mode conversion technique, also considered as a possibility for replacing the ECE method in STs, has likewise severe limitations. The location of the wave mode conversion ‘layer’, as well as the mode conversion efficiency, depend strongly on the local electron density gradient (∇n_e). Therefore, any spatial or time variations of the latter due to MHD events, for example, will introduce spurious effects in the $T_e(R,t)$ profile. The multi-energy SXR technique, on the other hand, uses the ratio of the power absorbed by multiple detectors, thus eliminating in theory any dependence on the magnetic field intensity and the electron density or its gradient. Therefore, this multi-energy capability has shown remarkable flexibility and could be used not only for fast electron temperature measurements [8-12], but also for impurity transport [13-15] and the study of slow macroscopic magnetohydrodynamic phenomena (e.g. RWMs, NTMs and the effect of 3D fields) [15,16].

In summary, imaging magnetically confined fusion plasmas in multiple energy ranges offers a unique opportunity of measuring simultaneously a variety of important plasma properties such as impurity concentrations (n_Z and Z_{eff}), electron temperature (T_e) and the appearance of non-Maxwellian ($n_{e,nM}$) tails. The two methods presently used lack either, space- and time-resolution in the case of the PHA measurements, or energy-resolution due to the use of a discrete number of metallic filters. The use of thin silicon detectors offers poor detection efficiency above 20 keV, introducing limitations for the study of non-Maxwellian tails generated by radio-frequency waves or the birth of runaway electrons. For this particular application, taking advantage of thicker detector slabs or high-Z materials is paramount.

II. New multi-energy PHA-imaging capability

The primary short-term goal is to design, build and operate a novel x-ray “pinhole” camera system to provide a time and space resolved 2D tomographic capability in multiple energy ranges simultaneously. The novel diagnostic technique proposed to be developed for tokamaks and stellarators will combine the best features from both PHA and multi-foil methods. This diagnostic will employ a pixelated x-ray detector in which the lower energy threshold for photon detection can be adjusted independently on each pixel of the detector. This configuration provides an unprecedented flexibility in the configuration of a multi-energy imaging x-ray detection system. The energy resolved measurements from this diagnostic can be used to produce images of both impurity concentrations (n_Z), from the absolute image intensity at different energy bands, and the electron energy distribution function, both thermal (T_e) and non-Maxwellian ($n_{e,nM}$), from the variation of emissivity with x-ray energy. High-Z impurity concentrations (e.g. molybdenum and tungsten) can also be derived from the intensity of the impurity peaks. ITER as we recall, has adopted beryllium as first wall and tungsten as divertor armor material, to reduce the tritium inventory an order of magnitude below that observed with carbon plasma-facing components (PFCs). In-lieu of the present requirements of modern tokamaks like JET, ASDEX-Upgrade and ITER, this diagnostic can provide a 2D distribution of the high-Z impurity emission and their asymmetries. The energy sensitivity offers also a unique opportunity to perform RF power deposition studies in plasmas without limitations on plasma performance.

The proposed system can image the plasma at the same toroidal angle with top-bottom and horizontal views [see Fig. 4-a)] using two Pilatus3 [17] x-ray cameras [see Fig. 4-b)]. The top-bottom view (not shown here) will complement the horizontal view for a full tomographic survey and will be of prime-importance for detecting in-out asymmetries in the emission from rotating high-Z impurities. A tangential view is preferable since in-out and top-bottom asymmetries can be simultaneously detected. A first proof-of-principle system in a radial configuration imaging the poloidal plane was deployed for testing at the Alactor C-Mod tokamak with excellent results [18]. At the heart of the new proposed system is a Pilatus detector which has been the detector of choice for various designs of x-ray crystal imaging spectrometers which our x-ray group at PPPL installed in NSTX, C-Mod, KSTAR, EAST, LHD [13-18], and in the future, NSTX-U, W7-X and ITER.

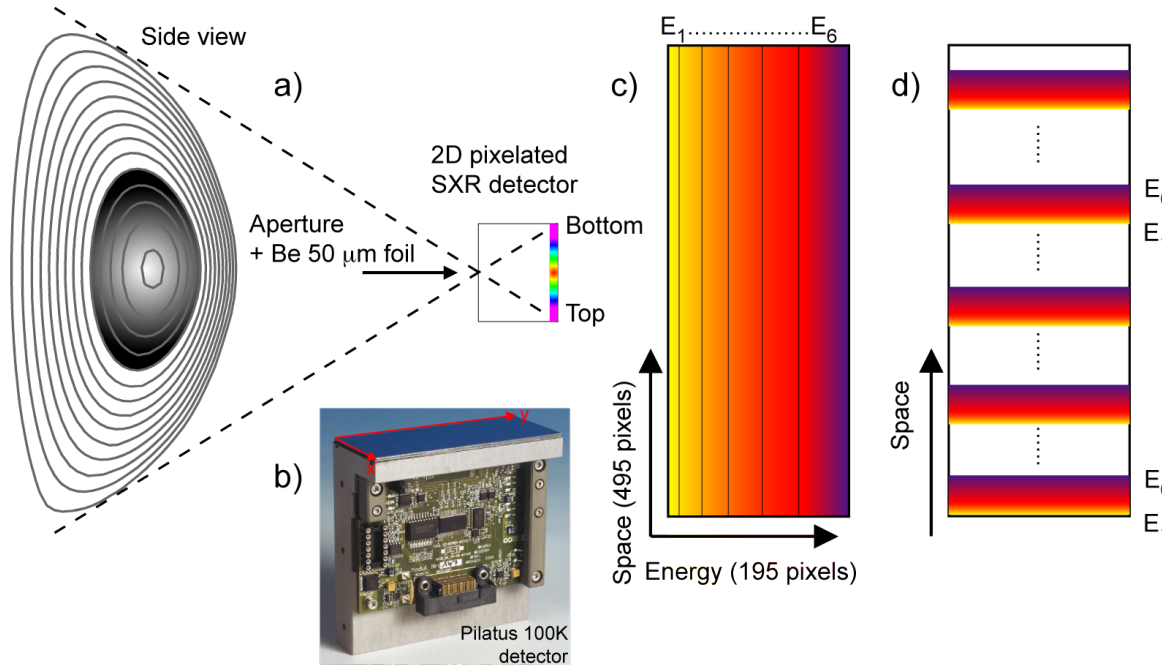


Fig. 4. Horizontal view for imaging PHA cameras envisioned for NSTX-U and DIII-D. The Pilatus 100K detector is shown in b), while two options for arranging the threshold energies are shown in c) and d), respectively.

The configurations of pixelated detectors can be optimized based on the Shannon-Nyquist sampling and interpolation theory [25], since the observed spectra are typically oversampled. A first configuration of choice is shown in Fig. 4-c). Since the x-ray emissivity is uniform along the toroidal magnetic field, the pixels in the same row sample the same plasma volume. It is therefore possible to obtain spectral resolution by setting the pixels in each row to varying energy thresholds, $E_1, E_2, E_3, E_4, E_5, E_6$, etc., where a larger number of pixels is set to the higher energy threshold to compensate for the exponential decrease of the photon intensity with energy. The optimized configuration [25], is shown in Fig. 4-d). Here, the entire detector area would be effectively used for each energy value, since by skipping pixel rows only redundant spatial information would be discarded. In summary, we plan to design, built and operate a novel energy resolving pinhole x-ray camera to provide, for the first time, a time and space resolved 2D

tomographic capability in multiple energy ranges, simultaneously. This diagnostic will adequately complement the diode-based or metallic-foil bolometer suites and contribute in constraining 2D time-history profiles of electron temperature, impurity density and plasma charge (Z_{eff}). A good measurement of Z_{eff} profiles is highly desirable and can be used in the calculation of the neoclassical conductivity, transport-induced by microscopic instabilities and the interpretation of non-inductive and inductive current fractions. The spatial and temporal resolutions will be adequate for MHD equilibrium, transport, RF power deposition, and slow MHD studies (e.g. resistive wall modes and the effect of 3D magnetic perturbations). Better time resolution can be obtained with the last version of the Eiger detector [17], which will have a framing rate of approximate 20 kHz. The potential for extracting valuable information from this self-contained x-ray system should be fully explored also as a possible burning plasma diagnostic (e.g. ITER and beyond). Finally, with minimal adjustment, this system could provide the backbone of “real-time” impurity density and temperature measurements, which could be fed to the plasma control system for feedback plasma control.

III. First tests in Alcator C-Mod

The first prototype tests were conducted on the Alcator C-Mod tokamak at the Plasma Science Fusion Center (PSFC) at the Massachusetts Institute of Technology (MIT). The Pilatus 100K x-ray camera was installed on a small radially viewing port viewing the plasma through a 50 μm thick beryllium vacuum window. A schematic of the configuration is shown in Fig. 5-a). The raw image of a plasma on Alcator C-Mod taken with the camera in the “metapixel” configuration -

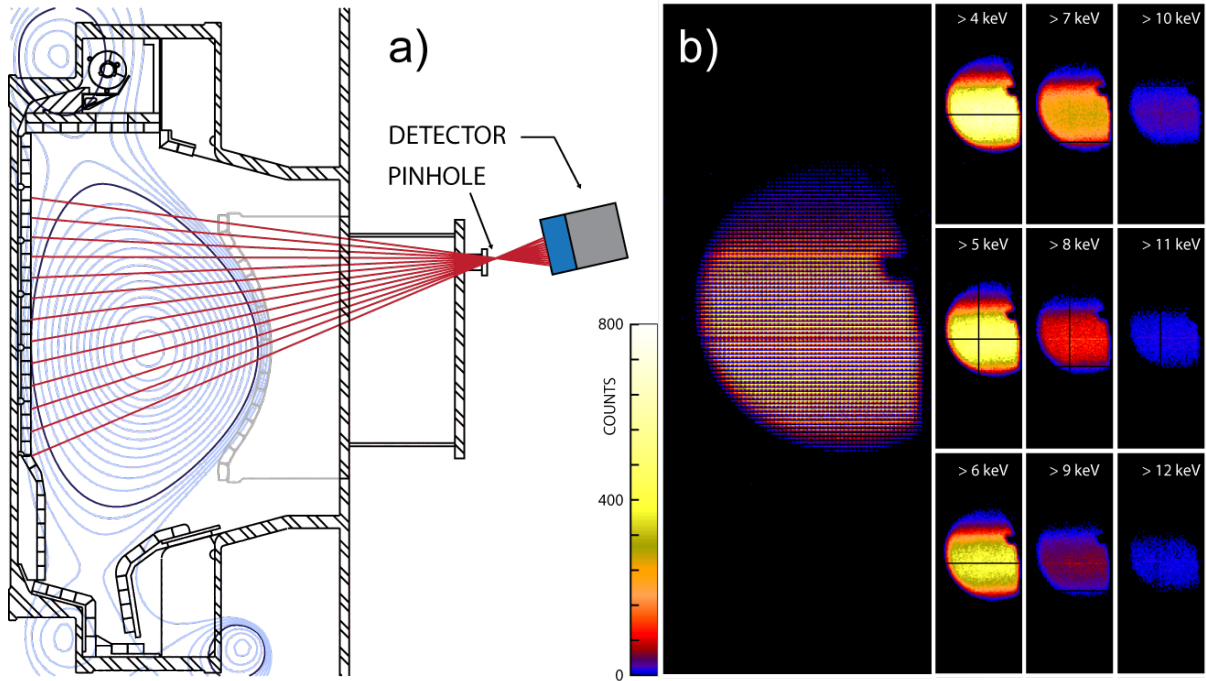


Fig. 5. a) Installation of imaging PHA-system in Alcator C-Mod (MIT-PSFC, see ref. [18]). b) Raw image using a 9-energy metapixel configuration is shown in b), while the nine-insets on the right-hand-side are created from the raw data by extracting the pixels with a given lower energy threshold.

with nine energy ranges: $E_{\min, \text{SXR}} > 4, 5, 6, 7, 8, 9, 10, 11$ and 12 keV - is shown in Fig. 5-b). This image was taken with an integration time of 2 ms (corresponding to a 5 ms framing rate). The nine-images on the right-hand-side of Fig. 5-b) are created from the raw data by extracting the pixels with a given lower energy threshold. The horizontal and vertical lines in the data correspond to space between the chips that make up the detector. This metapixel configuration is of preference for tangential-viewing systems. For viewing a toroidally symmetric plasma using a radial/poloidal view, such as that in NSTX-U, DIII-D and KSTAR, only 1D imaging is required. In this case the detector can be configured so that each column or row is given a different energy threshold as shown previously in Figs. 4-c) or -d), respectively. These configurations provide the best spatial resolution vertically, while still allowing a series of thresholds to be configured.

IV. Detection of effects introduced by non-Maxwellian tails (e.g. heating, current drive and birth of runaway electrons).

A good opportunity to obtain information on the velocity distribution function of energetic electrons is provided by the Bremsstrahlung emission. In particular, the forward scattering of Bremsstrahlung for relativistic electrons can be used to investigate the anisotropy of the distribution function, which is crucial for estimating the efficiency of the current drive or the birth of runaway electrons. Typically, for 20 keV electrons, the major part of the emission is in the forward direction, although the cone is not very narrow. However, for relativistic electrons with energies of 0.1-1 MeV, the emission is pointed strongly in the forward direction [26]. For energetic electrons with speed primarily along the magnetic field lines, we expect the x-ray emission to be strongly peaked in the direction of the toroidal field and opposite to the direction of the plasma current and thus a tangential view is preferable [27]; as mentioned above, a tangential view is also beneficial from the perspective of detecting in-out and top-bottom asymmetries simultaneously. Also, the possibility of dealing with runaway circulating electrons is one of the major ‘‘Achilles heels’’ for ITER and tokamak reactors. Therefore, the study of the birth of runaway electrons is crucial and the measurements of photons-energy in the range of 0.1-1 MeV are highly desirable.

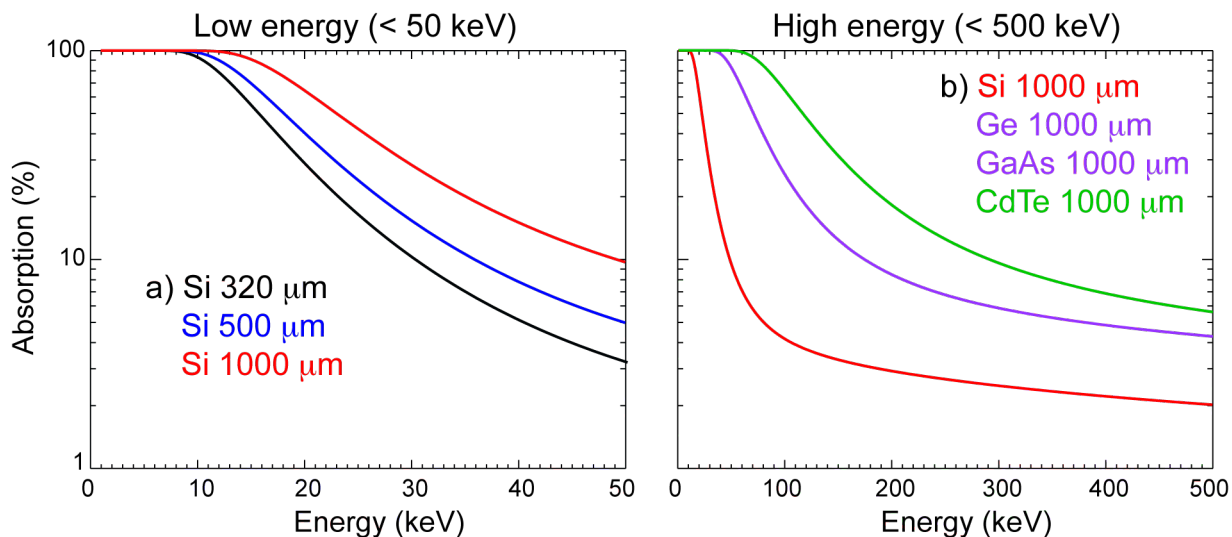


Fig. 6. a) Absorption coefficient for different thicknesses of silicon for energies below 50 keV. b) Greater efficiency at higher energy up to 500 keV is obtained using high-Z materials like Ge, GaAs and CdTe.

Silicon detectors are traditionally used due to the availability of good quality homogeneous material, and high charge carrier transport properties. However, 320 μm Si sensors offer detection efficiency less than 30% for energies above 20 keV and less than 5% above 40 keV due to its low atomic number ($Z = 14$) as shown in Fig. 6-a). The use of thicker (1 mm) silicon pixel array detectors would triple the efficiency at few tens of keV and will allow also the study of non-Maxwellian effects by probing higher x-ray energies up to 30-40 keV. The primary advantage of a higher-Z detector is its much greater efficiency since the photoelectric cross-section scales as Z^4 - Z^5 ; in comparison, the interaction cross sections for Compton scattering and pair production scale as Z and Z^2 , respectively. An optimum spectroscopic detector must favor photoelectric interactions and so semiconductor materials with a high atomic number are preferred. Therefore, the detection of higher-energy x-ray photons requires the use of Ge ($Z=32$), GaAs ($Z=31, 33$) and/or CdTe ($Z = 48, 52$) sensors to provide an adequate absorption as depicted in Fig. 6-b). For example, the efficiency for 1 mm Si detectors begins to fall above 10-20 keV, while for CdTe, efficiency is high up to 100 keV. This high-energy capability is of interest in our community especially when radio frequency waves (ECRH, ECCD and LHCD) heat plasmas introducing non-Maxwellian “tails” in the electron distribution function, which are prone to generate harder x-rays with energies up to 0.1-1.0 MeV. This is also the energy range of interest for hard x-rays expected in the study of the birth of runaway electrons. Dectris [17] has recently demonstrated the first 1 mm CdTe hybrid assembly detector array based on PILATUS with PILATUS 3 readout chip with large CdTe sensor units of 42x34mm for a minimum of dead space. The module shown in Fig. 7 has an active area is 83.8x33.6 mm^2 with nearly 100k (487x195) pixels and a pixel pitch (172 μm), identical to the Si-based detectors used by our group. These detectors will have less than 0.1% of defective pixels. In addition, each pixel will have a count rate stability better than 1%/min at 1×10^6 counts per second. These detectors will be tested and calibrated at PPPL this year and will become commercially available in 2015.



Fig. 7. New pixilated Pilatus3 CdTe detector. Courtesy of Dectris [17].

V. Summary.-

Multi-energy soft x-ray imaging of magnetically confined fusion plasmas provides a unique opportunity of measuring, simultaneously, a variety of important plasma properties such as medium- to high-Z impurity concentrations (n_z and Z_{eff}), electron temperature (T_e), and the appearance of suprathermal electrons in fusion plasmas. The use of thin silicon detectors offers poor detection efficiency above 20-30 keV and thus introduces limitations for the study of non-Maxwellian tails generated by radio-frequency waves or the birth of runaway electrons. In order to circumvent this limitation we propose using thicker Si detectors (~ 1 mm) or higher-Z materials such as Ge, GaAs or CdTe. This diagnostic system can also be used for the study of production of anisotropic hard x-ray distributions during electron runaway generation and its mitigation through massive gas and pellet injection. The potential for extracting valuable

information from this self-contained x-ray system should be fully explored also as a possible burning plasma diagnostic for inferring important plasma properties. With some adjustments for a burning plasma environment, these systems could provide the backbone of “real-time” impurity density and temperature measurements, which could also be fed to the plasma control system for feedback, positioning and control.

VI. References.-

- [1] E. H. Silver, *et al.*, Soft x-ray measurements from the PDX tokamak, *Rev. Sci. Instrum.*, 53, 1198, (1982).
- [2] K. W. Hill, *et al.*, Tokamak Fusion Test Reactor prototype x-ray pulse-height analyzer diagnostic, *Rev. Sci. Instrum.*, 56, 840, (1985).
- [3] K. W. Hill, *et al.*, Studies of Impurity behavior in TFTR, *Nucl. Fusion*, 26, 1131, (1986).
- [4] J. E. Rice, *et al.*, Continuum x-ray emission from the Alcator A tokamak, *Phys. Rev. A*, 25, 1645, (1982).
- [5] K. Molvig, *et al.*, Evidence for Magnetic Fluctuations as the Heat-Loss Mechanism in the Alcator Tokamak, *Phys. Rev. Lett.*, 41, 1240, (1978).
- [6] Z. Y. Chen, *et al.*, A compact soft X-ray PHA in the HT-7 tokamak, *Nuclear Instruments and Methods in Physics Research A*, 527, 604, (2004).
- [7] A. Czarnecka, *et al.*, Concept of pulse height analysis system (PHA) for Wendelstein 7-X, *Proceedings of the 38th EPS Conference on Plasma Physics*, Strasbourg, P1.052, (2011).
- [8] L. Delgado-Aparicio, *et al.*, A “multi-colour” SXR diagnostic for time and space-resolved measurements of electron temperature, MHD activity and particle transport in MCF plasmas, *Plasma Phys. Control. Fusion*, 49, 1245, (2007).
- [9] L. Delgado-Aparicio, *et al.*, Fast electron temperature measurements using a “multi- color” optical soft X-ray array, *Journal of Applied Physics*, 102, 073304, (2007).
- [10] L. Delgado-Aparicio, *et al.*, Soft x-ray continuum radiation transmitted through metallic filters: An analytical approach to fast electron temperature measurements, *Rev. Sci. Instrum.*, 81, 10E303, (2010).
- [11] K. Tritz, *et al.*, Compact “diode-based” multi-energy soft x-ray diagnostic for NSTX, *Rev. Sci. Instrum.*, 83, 10E109, (2012).
- [12] D. J. Clayton, *et al.*, Electron temperature profile reconstructions from multi-energy SXR measurements using neural networks, *Plasma Phys. Control. Fusion*, 55, 095015, (2013).
- [13] L. Delgado-Aparicio, *et al.*, Impurity transport studies in neutral beam heated spherical tokamak H-mode plasmas, *Nucl. Fusion*, 49, 085028, (2009).
- [14] D. J. Clayton, *et al.*, Multi-energy soft-x-ray technique for impurity transport measurements in the fusion plasma edge, *Plasma Phys. Control. Fusion*, 54, 105022, (2012).
- [15] L. Delgado-Aparicio, *et al.*, Impurity transport and effects on MHD in the National Spherical Torus Experiment (NSTX), *Nucl. Fusion*, 51, 083047, (2011).
- [16] L. Delgado-Aparicio, *et al.*, Soft x-ray measurements of resistive wall mode behavior in NSTX, *Plasma Phys. Control. Fusion*, 53, 035005, (2011).
- [17] See <https://www.dectris.com>
- [18] N. Pablant, *et al.*, Novel energy resolving X-ray pinhole camera on Alcator C-Mod, *Rev. Scientific Instrum.*, 83, 10E526, (2012).
- [19] A. Ince-Cushman, *Rotation Studies in Fusion Plasmas via Imaging X-ray Crystal Spectroscopy*, Ph. D. thesis, MIT, (2008).
- [20] A. Ince-Cushman, *et al.*, Spatially resolved high-resolution x-ray spectroscopy for

- magnetically confined fusion plasmas, *Rev. Sci. Instrum.* 79, 10E302, (2008).
- [21] K. W. Hill, *et al.*, A spatially resolving x-ray crystal spectrometer for measurement of ion-temperature and rotation-velocity profiles on the Alcator C-Mod tokamak, *Rev. Sci. Instrum.*, 79, 10E320, (2008).
- [22] E. Wang, *et al.*, Calculation of the Johann error for spherically bent x-ray imaging crystal spectrometers, *Rev. Sci. Instrum.*, 81, 10E329, (2010)
- [23] M. L. Reinke, *et al.*, X-ray imaging crystal spectroscopy for use in plasma transport research, *Rev. Sci. Instrum.*, 83, 113504, (2012)
- [24] L. Delgado-Aparicio, *et al.*, Effects of thermal expansion of crystal-lattice on x-ray imaging crystal spectrometer used in fusion research, *Plasma Phys. Control. Fusion*, 55, 125011, (2013).
- [25] E. Wang, *et al.*, Optimization of the configuration of pixelated detectors for the x-ray spectroscopy of hot plasmas based on the Nyquist-Shannon theorem, *Rev. Sci. Instrum.*, 83, 10E139, (2012).
- [26] S. von Goeler, *et al.*, Angular distribution of the Bremsstrahlung emission during lower hybrid current drive on PLT, *Nucl. Fusion*, 25, 1515, (1985).
- [27] S. von Goeler, *et al.*, Camera for imaging hard x rays from suprathermal electrons during lower hybrid current drive on PBX-M, *Rev. Sci. Instrum.*, 65, 1621 (1994).

The Princeton Plasma Physics Laboratory is operated
by Princeton University under contract
with the U.S. Department of Energy.

Information Services
Princeton Plasma Physics Laboratory
P.O. Box 451
Princeton, NJ 08543

Phone: 609-243-2245
Fax: 609-243-2751
e-mail: pppl_info@pppl.gov
Internet Address: <http://www.pppl.gov>